Spectral unmixing of multi-temporal data in gamma-ray spectrometry

Paul Malfrait, Jérôme Bobin, Anne de Vismes Ott

Spectral unmixing of multi-temporal data in gamma-ray spectrometry

Paul Malfrait[a], Jérôme Bobin[b], Anne de Vismes Ott[a,*], Jiaxin Xu[a]

[a] *IRSN/LMRE, Rue du Belvédère, 91400 Orsay, France*
[b] *CEA IRFU/DEDIP, 91191 Gif-sur-Yvette, France*

Abstract

A challenging problem in gamma-ray spectrum analysis is the rapid detection of artificial radionuclides at low activity levels. Until now, traditional methods focus on activity estimation based on single spectra, obtained by integrating over time the measured disintegration events. However, accounting for the well-constrained radionuclides decay should allow for a more accurate and sensitive activity estimation. For that purpose, we investigate a novel approach to estimate radionuclides' activity, which is i) first based on multi-temporal data, obtained from several short measurements rather than a single one, and ii) built upon a dedicated spectral unmixing, which allows processing multi-temporal data. The proposed algorithm allows accounting for both the full spectrum of each radionuclide (i.e. peaks and Compton continuum) and their activity decay in time. To that purpose, different approaches are investigated to model the temporal dependencies of the radionuclides' activities, and specifically to account for potentially out of equilibrium radionuclides' decay chains. Experimental results on both simulated spectra and real measurements are presented and compared to standard methods, it is shown that the proposed approach leads to more accurate estimations and faster detection of artificial radionuclides.

Keywords: gamma-ray spectrometry, model, full spectrum analysis, Poisson

*Corresponding author
Email address: anne.de-vismes@irsn.fr (Anne de Vismes Ott)

statistics-based spectral unmixing, metrological analysis

1. Introduction

Gamma-ray spectrometry is one of the major techniques used to measure the activity concentrations of radionuclides in environmental samples. One of the main challenges raised by radioactivity measurement is the rapid analysis of samples in case of an incident or an accident with releases. This task mandates fast measurements as well as rapid and reliable information to the population Knoll (2010).

The main challenges of γ-ray spectra analysis lies in: i) the rapid detection and identification of the radionuclides which can be detected from the sample and ii) the accurate estimation of the radionuclides' activities. This is a particularly tricky challenge when the statistics of the counting rate is low. This has attracted a lot of attention in the field of rapid detection and rapid characterization of sources under emergency conditions.

1.1. Measurement of radioactivity in the air

In the present study, and without loss of generality of the proposed method, we will focus on the analysis of the aerosol samples measured at IRSN [1] for validation purposes. More precisely, as part of its monitoring brief, IRSN carries out regular measurements of radioactivity levels in the environment, employing high-performance investigation means for the quantification of trace amounts.

As part of the OPERA-Air network (permanent radioactivity observatory), the data measured at IRSN also serves as a support to the numerous research and expertise studies on the time and spatial variations of radionuclides in the environment. This paper focuses on the 10 high flow air samplers (300-900 m3.h-1), whose filters are sampled and measured by gamma-ray spectrometry

[1] `https://www.irsn.fr/`

on a weekly basis. In this way detection of very low concentrations of abnormal artificial radionuclides may indicate low-magnitude incident releases or accident releases at remote places.

In case of emergency, rapid and reliable information to the population is required while a low level measurement would help the source term assessment. During the passage of the contaminated air masses from the Fukushima accident over France (de Vismes Ott et al. (2013)) each sampled air filter was measured twice to meet both purpose: a short measurement just after sampling and a long measurement few days later. Indeed, the spectrum of the early measurement is contaminated by the presence of the particulate radon progeny sampled by the filter, which gives rise to many peaks and a high background as shown on Figure 1. The second spectrum on Figure 1 was obtained by the long (4 days) measurement 4 days after sampling : all the short half-lived radon progeny have vanished and the simpler spectrum containing only few radionuclides (^{7}Be, ^{210}Pb, ^{40}K and ^{22}Na in decreasing activity concentration order) make possible the detection of ^{137}Cs and its quantification at trace level (0.1 µBq.m^{-3}). The routine measurements of the aerosol filters being performed one week after sampling and for 3 days, the determination of ^{137}Cs, and consequently the detection of other potential artificial radionuclide, takes two weeks once the filter is sent to the metrology laboratories. The objective is therefore to improve the gamma-ray spectrum analysis and to particularly focus on artificial radionuclides at low statistics.

1.2. State-of-art for gamma-ray spectra analysis

In a nutshell, a gamma-ray spectrum records the histogram of the number of detected events as a function of the energy deposited by the gamma-ray or X-ray in the detector. The interactions between the photons and the material of the detector for a mono-energetic source lead to a spectrum with two main components: a peak at the photon energy, called total absorption peak or full energy peak, and a Compton continuum (see Knoll (2010) and Gilmore (2001)

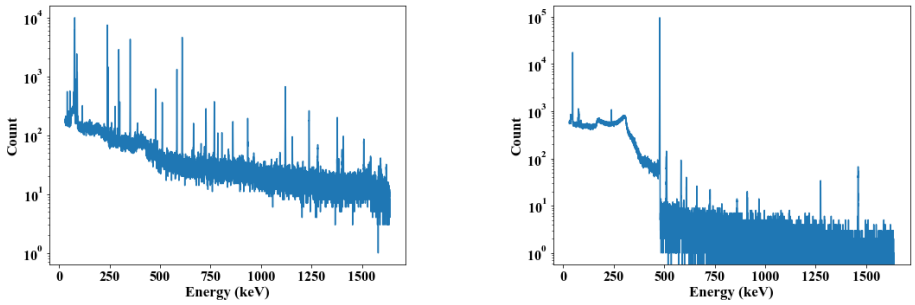

Figure 1: Examples of gamma-ray spectra of two measurements of an aerosol filter : half-an-hour long measurement performed half an hour after sampling (left panel), and a 3 days and 17h long measurement performed 4 days after sampling (right panel).

for precision). Depending on its decay scheme, a radionuclide can emit photons with different energies. This yields a characteristic spectrum for a radionuclide with several peaks and associated continua. The total measured spectrum is then the linear combination of the individual spectra of each radionuclide and a background spectrum.

Classical analysis methods identify and quantify the radionuclides from their characteristic energy peaks. In these approaches, after identification of the radionuclides thanks to characteristic emissions, their activity is computed from the peak area, via the detection efficiency (*e.g.* Genie2000 from Canberra Mirion-Canberra (2016)). This process is usually based on Region of Interest (ROI) analysis, as described in Gilmore (2001). However, these methods are rather limited: the calculation of the peak areas implicitly assumes that the counting distribution is Gaussian. This is generally not a valid assumption, especially at low statistics. In this regime, radioactive sources emit photons randomly according to a Poisson process. In complex samples, radionuclides may overlap, leading to interferences between individual spectra. These samples are very difficult to analyse with peak-based analysis since it requires accounting for the photon peaks as well as Compton continua. Let us notice that peak-based analysis has been generalized Kirkpatrick and Young (2009) to account for the

exact Poisson statistics of the data. It is interesting to point out that this study demonstrated the need to account for the exact statistics of the measurement. Nevertheless, these methods do not account for the whole information carried by the full spectrum since they rely on region of interest at the vicinity of related peaks.

Further accounting for the full-spectrum information in gamma-ray spectrum analysis has been advocated in Hendriks et al. (2001). In this article, the authors demonstrated that, compared to the standard peak-based analysis, using the full spectrum improves the sensitivity and reduces the time of measurement. However, these investigations make use of a re-weighted least squares method, which is not fully adapted to account for the Poisson statistics of the data.

Activity estimation problem in gamma-ray spectrometry has been also studied in Sepulcre et al. (2013), considering activity estimation as a sparse regression problem. In this article, the authors propose to estimate the number of individual electrical pulses and their arrival times. Other contributions of the activity estimation in the field of machine learning algorithms were also applied to gamma-ray spectrum analysis as presented in Yoshida et al. (2002), where peak energy data are applied to neural networks. In Sharma et al. (2012), machine learning algorithm was applied for the detection of anomaly events in gamma-ray spectra. Based on conventional neural networks, these approaches do not however allow to account for the precise physical model underlying the detection process.

In Xu et al. (2020), we introduced the first full spectrum analysis method which allows to account for the Poisson statistics. In this paper, we particularly showed the advantage of making profit of all the information that full spectrum bears, leading to a more accurate and sensitive activity estimation procedure. This method has further been validated with real aerosol samples in section 5. In this paper the model for a spectrum $x = [x_1, \cdots, x_M]$ is composed of M energy channels and is described as follows:

$$\forall c = 1, \cdots, M; \quad x_c = \sum_{n=1}^{N} \phi_{nc} a_n + b_c, \tag{1}$$

where $\phi_n = [\phi_{n1} \cdots, \phi_{nc}]$ stands for the spectral signature of the n-th radionuclide and b_c for the background in channel c. The activities $\{a_n\}_{n=1,\cdots,N}$ are estimated from the analysis of a single spectrum of a long measurement. We recently improved the method to better calibrate the simulated spectral signatures (Xu et al. (2022b)) which proves to be necessary because of the detector's variability that may cause slight shifts in the energy calibration of the measured spectrum, this allows to precisely match the simulated signatures to the observed spectrum so that the estimation is not biased by the detectors' energy calibration. The characteristic limits of the unmixing algorithm are also explored, as the standard peak based techniques could not be used to determine decision thresholds and detection limits via spectral unmixing. The results of Xu et al. (2022a) allows us to compute them directly without having to rely on Monte-Carlo simulation in order to estimate them. The aim of this paper is to use the same unmixing idea but to apply it on multiple spectra to get earlier estimations of the activities. The joint estimation will be performed on multiple consecutive measurements of the same sample, allowing us to use the disintegration model of the radionuclide to get a quicker activity estimation.

1.3. Multi-temporal gamma-ray spectrometry

The traditional measurement process consists in acquiring a single spectrum which is obtained as an integrated spectrum during a certain amount of time. For the sake of accuracy, the acquisition time is generally taken long (from two days up to a week) and after a decay period to let the short-lived radionuclides disappear before the measurement. This allows for the short-lived radionuclides to vanish while providing more statistics to improve the detection of long-lived radionuclides present at low level, such as ^{137}Cs or ^{22}Na. The activity of the radionuclides of interest in the environment survey are very low with respect to the activities of short-lived radionuclides as ^{214}Pb/Bi, ^{208}Tl or ^{212}Pb/Bi which

can interfere in the estimation. The activity of the radionuclides usually observed in aerosol samples is presented in 2. This largely hampers the ability to rapidly detect artificial radionuclides which could trace for incidents or accidents. The aim of this paper is to build a temporal model that cope with these short-lived radionuclides and is able to detect the low-level radionuclides earlier than the usual week of measurement.

In fact, making use of the time decay of the radionuclides should provide extra information to better discriminate between the radionuclides to be identified. Therefore, we propose a different strategy where the measurements are acquired on multiple, shorter time intervals. This leads to multiple snapshots of the same sample taken in different consecutive time intervals. This further allows taking advantage of the time dependency between these multiple measurements to perform a joint analysis on a sample measured multiple times.

More formally, the variation in time of each of the radionuclides can be described by the following physical time decay model:

$$A_n(t) = a_n(0)e^{-\lambda_n . t}, \tag{2}$$

where $A_n(t)$ is the number of nuclear disintegrations per second for the n-th radionuclide at time t, $a_n(0)$ its activity at the beginning of the measurement and λ_n the decay constant of the radionuclide. Let's define by A_n the total activity of the n-th radionuclide during the s-th segment ($s = 0, ..., S$) between time t_s and t_{s+1} as follows :

$$\begin{aligned} A_n &= \int_{t_{s-1}}^{t_s} A_n(t)dt & (3)\\ &= \int_{t_{s-1}}^{t_s} a_n(0)e^{-\lambda_n t}dt & (4)\\ &= a_n(0)\psi_{sn}, & (5) \end{aligned}$$

where the constant ψ_{sn} is defined as:

$$\psi_{sn} = \int_{t_{s-1}}^{t_s} e^{-\lambda_n t} dt \tag{6}$$

In the next, and for simplicity, the activity $a_n(0)$ of each radionuclide will be denoted by a_n, which will be the quantity of interest to be estimated from the measurements.

A gamma-ray spectrum measured between time t_{s-1} and t_s is then defined as the linear combination of each of the N radionuclides spectral signatures ϕ_n ($i.e.$ the detector's response in energy for a single radionuclide - see Xu et al. (2020), a signature for a radionuclide is obtained by normalizing the spectrum by the measurement time and the activity of the source), to which a background term $\mathbf{b}$ is added (of dimension $1 \times M$, M being the number of channels of the spectrum). The measurement background is the blank spectrum which is obtained by leaving the detector empty during the acquisition process. The spectrum for the s-th segment and energy channel i is then described as follows:

$$x_{sc} = \sum_{n=1}^{N} a_n \psi_{sn} \phi_{nc} + b_{sc} \tag{7}$$

where $b_{sc} = (t_s - t_{s-1}) b_c$

Finally, the spectrum is subject to Poisson noise due to the counting process of the detection. Defining y_{sc} as the measured spectrums in the s-th time segment and i-th energy channel, the final model is :

$$y_{sc} \sim Poisson\Big(\sum_{n=1}^{N} a_n \psi_{sn} \phi_{nc} + b_{sc} \Big) \tag{8}$$

where the measured spectrum is a random realization following a Poisson distribution with mean x_{sc}.

1.4. Contribution

In this paper, we investigate a new approach for the estimation of the activity of radionuclides from multiple gamma-ray spectra. Firstly, it builds upon the joint analysis of gamma-ray spectra measured in consecutive time intervals.

This allows to account for the radionuclides' activity decay, which bears information to better distinguish between them. Secondly, we introduce a novel spectral unmixing algorithm to tackle multi-temporal measurements and which is based on a recently introduced method Xu et al. (2020). In contrast to standard methods that perform on single measurements, we propose to investigate two distinct models for the time dependency of the radionuclides' activity : i) the first one assumes that all the radionuclides are in equilibrium, and ii) the second one allows accounting for the presence of radionuclides that are not in equilibrium. In the latter, the method allows taking into consideration the correlation between parent and daughter radionuclides activities, as described in Bateman (1910). These models are detailed in Section 2. Section 3 details the proposed multi-measurements spectral unmixing method. In Section 4, the proposed method is applied to simulated spectra, to assess the accuracy of the proposed models and algorithms. Next, experimental results on real spectra are presented in Section 5. We particularly show that accounting for time-dependency in multiple γ-ray spectra allows for a faster detection of the radionuclides present in the data while preserving a good accuracy of the estimation of their activities.

2. Modelling multi-measurements γ-ray spectrometry data

Accounting for temporal information in spectral unmixing first requires designing dedicated models to describe multi-temporal gamma-ray spectra. To that purpose, we hereafter focus on various models for multi-temporal γ-ray spectra, with increasing complexity.

Without loss of generality, these models will be illustrated with a sequence of γ-ray spectra, for which both simulations and real measurements are available. These data originate from an aerosol sample which has been measured with a HPGe detector. They are composed of 11 measurements covering a total time of almost 8 days (670 800 s). As displayed in Figure 2, time intervals of various lengths have been chosen. The starting point has been taken 30 minutes after the end of the sampling process, this is due to the sample preparation process:

the aerosol filter is pressed into pellets before being put on the detector. More details about the detector setup is given in Appendix A.

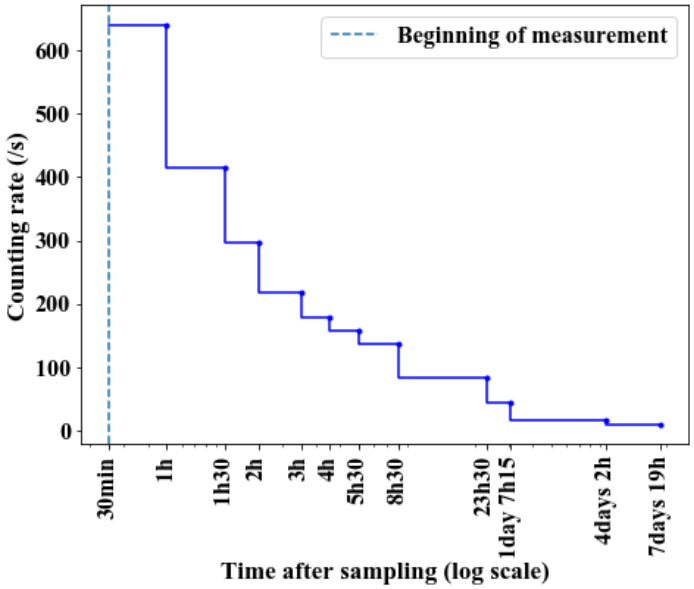

Figure 2: Temporal scheme of measurement used in this paper.

Accounting for the time correlations in γ-ray spectra builds upon a good understanding of the activity of the radioactive series of radionuclides. More precisely, when radionuclides are in the same radioactive sequence and the half-life of the parent radionuclide is longer than the half-life of the daughter radionuclide, the parent's activity affects the daughter's. In fact, any radionuclide sequence is described by Bateman's equation which relates the activity of a daughter radionuclide in terms of its rate λ_d, its activity at $t = 0$, $a_d(0)$, and its parent rate λ_p and abundance $a_p(0)$ (see Bateman (1910) for more details) :

$$a_d(t) = a_d(0)e^{-\lambda_d t} + \frac{\lambda_p}{\lambda_d - \lambda_p} a_p(0)\left(e^{-\lambda_p t} - e^{-\lambda_d t}\right) \tag{9}$$

As an illustration, let us consider the ^{214}Pb - ^{214}Bi chain :

$$^{214}Pb(27min) \longrightarrow ^{214}Bi(20min)$$

Segment	Start time	Duration
1	30min	1 800s (30min)
2	1h	1 800s (30min)
3	1h30	1 800s (30min)
4	2h	3 600s (1h)
5	3h	3 600s (1h)
6	4h	5 400s (1h30)
7	5h30	10 800s (3h)
8	8h30	54 000s (15h)
9	23h30	28 000s (∼7h45)
10	∼1 day 7h15	240 000s (∼2 days 19h)
11	∼4 days 2h	320 000s (∼3 days 17h)

Table 1: The temporal scheme of the measurement used throughout this paper.

In this case, the half-life of the parent radionuclide is of the same order of magnitude as the daughter's half-life: $t_{parent} \approx t_{daughter}$. For this disintegration chain, the correlation between the activity of the parent and daughter radionuclide can be described with Bateman's equation and the activity of ^{214}Pb will participate in the activity of ^{214}Bi.

As a second example, let us consider the radioactive series composed of ^{212}Pb, ^{212}Bi and ^{208}Tl, which can be described as follows:

$$^{212}Pb(10.6h) \longrightarrow ^{212}\ Bi(61min) \longrightarrow ^{208}\ Tl(3min)$$

In this chain, each radionuclide disintegrates in a descendant with a much shorter period. Thus, Bateman's equation is simpler as $\frac{\lambda_p}{\lambda_d - \lambda_p}$ is close to 0 in the equation 9. Moreover, the daughter radionuclides ^{212}Bi and ^{208}Tl are considered at equilibrium with their parent and have the same decreasing rate as ^{212}Pb. All the daughter radionuclides that disintegrate derive directly from a

parent radionuclide which has previously disintegrated itself. Indeed, the daughter radionuclides cannot decay faster than they are produced and thus depend on the decay rate of ^{212}Pb.

In the next sections, we describe different multi-temporal models for each of these two families and with or without the Bateman's equation simplification for the ^{214}Pb-^{214}Bi decay series.

Model for multi-temporal γ-ray spectra in equilibrium

The first model to be considered is dedicated to the decay series which are at secular equilibrium. This model will be composed of different quantities, which are summarized below :

- a_n : the activities $a_n(0)$ for each of the N radionuclides (a vector of size N)
- ϕ_{nc} : the spectral signature of the n-th radionuclide in the c-th energy channel.
- ψ_{sn}: the temporal signatures of the n-th radionuclide in the s-th time segment, described in Equation 6.
- b_c is the background in the c-th energy channel. It originates from cosmological or telluric γ activity. It is assumed to be constant during the acquisition time so that the background for a given time interval is defined as $(t_s - t_{s-1})b_i$.

Throughout this article, the spectral signatures $\{\phi_{nc}\}_{n,c}$ are assumed to be known as it represents the energy signature of the radionuclide. It can be derived from measurements of a standard source containing a single radionuclide. However, this can only apply to radionuclides, for which a standard source can be made. This is not the case for some of the radionuclides that can be identified in aerosol samples. For that purpose, we rather compute the spectral signatures from simulations (see Appendix A).

The model for the radionuclides when we approximate the Bateman's equation's second term by 0 is described as follows:

$$\forall s = 1, \cdots, S; c = 1, \cdots, c; \quad x_{sc} = \sum_{i=1}^{N} a_n \psi_{sn} \phi_{nc} + b_{sc} \tag{10}$$

where the background is given by $b_{sc} = \delta_s b_c$. The quantity δ_s stands for the time duration of the s-th measured spectrum.

Model for multi-temporal γ-ray spectra with Bateman's equation

In the previous section, the temporal signatures do not model for possible out of equilibrium radionuclides. The term ψ associated to the activities in a disintegration family considers that the daughter radionuclides are decreasing with the period of their parent. To further deal with the radionuclides whih are not in equilibrium, it is necessary to introduce an extra term : ψ_s^B, modelling the interaction between the daughter and its parent radionuclide, such as with the ^{214}Pb/^{214}Bi family. This extra factor takes into account the activity of the parent radionuclide but will have an impact the daughter's activity. This is described by Bateman's equation (Section 2) :

$$a_d(t) = a_d(0)e^{-\lambda_d t} + \frac{\lambda_p}{\lambda_d - \lambda_p} a_p(0)\big(e^{-\lambda_p t} - e^{-\lambda_d t}\big) \tag{11}$$

which models for the relationship between the parent and daughter radionuclides. The expression of the extra term ψ_s^B is then defined as follows :

$$\begin{aligned} \psi_s^B &= \frac{1}{a_p(0)} \int_{t_{s-1}}^{t_s} \frac{\lambda_p}{\lambda_d - \lambda_p} a_p(0)\big(e^{-\lambda_p t} - e^{-\lambda_d t}\big) dt \\ &= \frac{\lambda_p}{\lambda_d - \lambda_p} \Big(\int_{t_{s-1}}^{t_s} e^{-\lambda_p t} dt - \int_{t_{s-1}}^{t_s} e^{-\lambda_d t} dt \Big) \end{aligned} \tag{12}$$

Without loss of generality, the model in Eq.(10) for a disintegration family of two radionuclides a parent and its daughter reads as:

$$\forall s = 1, \cdots, S; c = 1, \cdots, c; \quad x_{sc} = \sum_{i=1}^{N} a_n \psi_{sn} \phi_{nc} + a_m \psi_{s,j}^{(B)} \phi_{j,c}^{(B)} + b_{sc} \tag{13}$$

In the next section, we will investigate how these models can be used to design spectral unmixing algorithms that are specifically tailored to analyse multi-temporal measurements.

3. Spectral unmixing algorithms for multi-temporal measurements

3.1. Statistical modeling

In this section, we introduce a new spectral unmixing algorithm to analyse multi-temporal measurement in gamma-ray spectrometry. For that purpose, we first need to define an estimator for the mixing weights of the mixture model that describes γ-ray spectra. Let us recall that, for each channel $m = 1, ..., M$ and time segment $s = 1, ..., S$, the general expression for the mixture model is of the form :

$$\forall s = 1, \cdots, S; c = 1, \cdots, c; \quad x_{sc} = \sum_{n=1}^{N} a_n \psi_{s,n} \phi_{nc} + \delta_s b_c \tag{14}$$

This expression gives the average number of counts per energy channel and time interval. The actual measurement follows a Poisson distribution, which can be formalized as follows:

$$\begin{aligned} \forall s = 1, \cdots, S; c = 1, \cdots, c; \quad y_{sc} &\sim Poisson(x_{sc}) \\ &\sim \frac{x_{sc}^{y_{sc}} \exp x_{sc}}{y_{sc}!} \end{aligned}$$

Since the channels and time segment are statistically independent, the likelihood with respect to the complete multi-temporal measurements is given by:

$$\mathcal{P}(\{y_{sc}\}_{s,c} | \{x_{sc}\}_{s,c}) = \prod_{s=1}^{S} \prod_{m=1}^{M} \frac{x_{sc}^{y_{sc}} \exp(x_{sc})}{y_{sc}!} \tag{15}$$

It is then customary to take the log to simplify the expression by defining the negative log likelihood:

$$L(\{y_{sc}\}_{s,c} | \{x_{sc}\}_{s,c}) = \sum_{s,c} x_{sc} - y_{sc} \log(x_{sc}) + \log(y_{sc}!) \tag{16}$$

Since, the model only depends on the unknown activities $\{a_n\}_n$, and following Xu et al. (2020), we take the negative log likelihood and add an extra constraint to enforce the non-negativity of the mixing weights:

$$\{\hat{a}_n\}_n = \text{argmax}_{a\geq 0} L(\{y_{sc}\}_{s,c}|\{a_n\}_n) \quad (17)$$

$$= \text{argmax}_{a\geq 0} \sum_{s,c} x_{sc} - y_{sc}\log(x_{sc}) \quad (18)$$

where $\log(y_{sc}!)$ is omitted since it is constant and each term x_{sc} is a function of the activities $\{a_n\}_n$ according to models (10) or (13).

The problem in Equation 17 does not admit a closed-form expression and must be evaluated using a minimisation algorithm. The main challenge is that the presence of the non-negativity constraint makes this problem non-differentiable. A traditional gradient descent algorithm cannot be adopted. Fortunately, different types of algorithms can be used, such as primal-dual algorithms (see Chambolle and Pock (2011); Xu et al. (2020)) or the multiplicative update algorithm (see Lee and Seung). Primal-dual algorithms offer a highly flexible framework at the cost of the need for tuning extra hyperparameters (see Xu et al. (2020) for more details). For its simplicity, we rather focus on extending the multiplicative update algorithms to multi-temporal measurements.

3.2. The multiplicative update algorithm and its extension to multi-temporal data

In this section, we introduce a spectral unmixing algorithm, based on the multiplicative update algorithm, which is tailored to the three distinct models we introduced in Section2:

- Model "without time" : Segment by segment analysis, no time correlation, we analyse the whole spectrum and estimate the activity in each temporal segment using the algorithm developed in Xu et al. (2020).

- Model "equilibrium hypothesis" : we benefit from temporal information with the joint analysis of the multi-temporal measurements. This amounts

to use the temporal signatures to model for the time dependencies. In this model, every disintegration family is assumed to be at secular equilibrium.

- "Bateman" model : This model makes use of Bateman's equation to model for the temporal dependencies that are not in secular equilibrium.

In each model the algorithm is based on the non-negative matrix factorization (Lee and Seung) the difference lies in the update of the activities. We will now present the most complex case of "Bateman" model as the others deduct directly from this one.

The multiplicative update algorithm first builds upon a gradient-based minimisation scheme. The derivative of the negative log likelihood with respect to each mixing weight a_n is given by :

$$\frac{\partial X_{sc}}{\partial a_n} = \psi_{sn}\phi_{nc} + \phi_{nc}\psi_{sn}^{(B)} \tag{19}$$

If the n-th radionuclide is not in a radioactive series, then $\psi_{sn}^{(B)} = 0$ and the second term disappears. This then builds down to:

$$\frac{\partial L(\{y_{sc}\}_{s,c}|\{x_{sc}\}_{s,c})}{\partial a_n} = \sum_{s,c}\left(\psi_{sn}\phi_{nc} - \frac{\psi_{sn}\phi_{nc}y_{sc}}{x_{sc}}\right) \tag{20}$$

Following Lee and Seung, the update rule of the multiplicative update algorithm can be obtained by zeroing the derivative of the negative-log-likelihood with respect to each mixing weight. The main difference between all the mixture models lies in the structure of the temporal signatures, which embeds the temporal information and is dependent on the temporal scheme of the measurements. The update rule for each model is defined as follows for each step k of the algorithm:

- Model "without time" : each time segment is processed independently, the activities of the sought-after radionuclides are then dependent on the time segment s, which yields multiple estimations of the activities $\{a_{sn}\}_{s,n}$.

The resulting update rule then reads:

$$a_{sn}^{(k+1)} = a_{sn}^{(k)} \frac{\sum_{c=1}^{M} \phi_{nc} y_{sc}/x_{sc}}{\sum_{c=1}^{M} \phi_{nc}}, \tag{21}$$

where $x_{sc} = \sum_{n=1}^{N} \phi_{nc} a_{sn}^{(k)} + b_{sc}$. This is similar to the update rule of the algorithm proposed in André et al. (2020).

- Model "equilibrium hypothesis" : does include the temporal signatures, but approximates the Bateman's term as 0:

$$a_{n}^{(k+1)} = a_{n}^{(k)} \frac{1}{\sum_{s=1}^{S} \psi_{sn} \sum_{c=1}^{M} \phi_{nc}} \sum_{s,c} \psi_{sn} \phi_{nc} y_{sc}/x_{sc} \tag{22}$$

where $x_{sc} = \sum_{n} \psi_{sn} \phi_{nc} a_{n}^{(k)} + b_{sc}$. The mixing weights are estimated considering that every decay series are at secular equilibrium.

- "Bateman" model : This model includes Bateman's equation for decay series which are not in equilibrium (*i.e.* for instance ^{214}Pb/ ^{214}Bi parent/daughter chain). The multiplicative update rule is then defined as follows:

$$a_{p}^{(k+1)} = a_{p}^{(k)} \frac{\sum_{s,c} \left(\psi_{s,p} \phi_{p,c} + \psi_{s,d}^{(B)} \phi_{d,c} \right) y_{sc}/x_{sc}}{\sum_{s=1}^{S} \psi_{s,p} \sum_{c=1}^{M} \phi_{p,c} + \sum_{s=1}^{S} \psi_{s,d}^{(B)} \sum_{c=1}^{M} \phi_{d,c}} \tag{23}$$

where a_p (resp. $\psi_{p,c}$ and $\phi_{p,c}$) stands for the parent activity (resp. its temporal and spectral signatures), $\psi_{s,d}^{(B)}$ stands for the corresponding Bateman temporal signature and $\phi_{d,c}$ is the associated daughter spectral signature. The current estimate of the mixture model is given by $x_{sc} = \sum_{n} \psi_{sn} \phi_{nc} a_{n}^{(k)} + b_{sc} + a_{p}^{(k)} \psi_{s,d}^{(B)} \phi_{d,c} + b_{sc}$. The mixing weights of the radionuclides that are in secular equilibrium are updated as in Model "Equilibrium hypothesis".

These update rules are performed sequentially until convergence is reached. The stopping criteria we impose to our algorithm is to stop when the relative variation of $A^{(k)}$, which is defined by:

$$\frac{\sum_n (a_n^{(k+1)} - a_n^{(k)})^2}{\sum_n {a_n^{(k)}}^2} \leq \epsilon \tag{24}$$

is smaller than value $\epsilon = 10^{-6}$. The maximum number of iterations is fixed to $K = 2000$ iterations.

4. Numerical experiments with simulated data

Radionuclide	Half life	Activity (Bq)
^{7}Be	$53,22$ days	420
^{22}Na	$2,60$ years	0.10
^{40}K	$1,265.10^{9}$ years	1.9
^{137}Cs	$30,05$ years	0.020
^{210}Pb	$22,3$ years	27
^{228}Ac	$14,02.10^{9}$ years (period of the ^{232}Th)	0.075
^{208}Tl	$3,06$ minutes	219
^{212}Bi	$60,54$ minutes	635
^{212}Pb	$10,64$ hours	481
^{214}Bi	$19,9$ minutes	2164
^{214}Pb	$26,8$ minutes	861

Table 2: List of simulated radionuclides with their half-life and activity.

4.1. Description of the simulations

In order to simulate a spectrum similar to the one we obtain in the environmental monitoring, we use the previous models and simulate the most common radionuclides in the samples we usually gather. The radionuclide dictionary will then be : ^{7}Be, ^{22}Na, ^{40}K, ^{137}Cs, ^{210}Pb, ^{228}Ac, ^{212}Pb, ^{212}Bi, ^{208}Tl, ^{214}Pb and ^{214}Bi. As previously seen, the ^{212}Pb, ^{212}Bi, ^{208}Tl series is considered at secular

equilibrium. Bateman's equation is used to model the activities of ^{214}Pb and ^{214}Bi. Indeed, as the disintegration periods of these two radionuclides are very similar, the secular equilibrium approximation won't hold in practice, as seen in 2. These simulations will be used to illustrate the differences between the unmixing algorithms and the importance of the theoretical knowledge carried out by the choice of the temporal models.

In order to simulate gamma-ray spectra, we make use of the mathematical model described in 2, and precisely described as follows:

$$x_{sc} = \sum_n a_n \psi_{sn} \phi_{nc} + \phi_{^{214}Bi,c} \psi_s^{(B)} a_{^{214}Pb} + b_{sc} \tag{25}$$

where,

- the term ϕ_{nc} stands for the spectral signatures of the n-th radionuclide in the channel c, which are computed thanks to MCNP-CP simulations. This software allows simulating the response of the HPGe detector used for measurements, as if standard sources were used for each radionuclide. We refer the reader to Appendix A for more details about the simulations.

- The activities $\{a_n\}_n$ of the radionuclides are chosen to be close to a real aerosol sample. The levels are presented in table 2.

- the temporal signatures $\{\psi_{sn}\}_{s,n}$ are computed according Equation 6. The duration of the time intervals are presented in table 1.

- The term $\psi_s^{(B)}$ corresponds to the temporal signature of ^{214}Pb as defined in Equation 12.

- The background b is a real measurement, realized with the empty HPGe detector used in the laboratory over a long time (typically one week). It is customary to take such a spectrum as background for the analysis that we carry in the laboratory. The background spectrum is then reduced to the background per second (by dividing by the counting time) and multiplied by the counting time of the segments we are using.

As can be seen in top-left panel of Figure 3, the simulated radionuclides have different behaviours through time. Three categories can be distinguished. The first one corresponds to the long-lived radionuclides :^{7}Be, ^{22}Na, ^{40}K, ^{137}Cs, ^{210}Pb, ^{228}Ac. The activities of these radionuclides are mostly constant over time since their periods are much greater than a week. The activities of these long-lived radionuclides vary quite significantly from few mBq for ^{137}Cs to 420 Bq for ^{7}Be allowing us to compare the performances of the models at low and higher activities. The second category is composed of the ^{212}Pb, ^{212}Bi, ^{208}Tl decay chain which is considered at secular equilibrium. These radionuclides have short half-lives (6 minutes up to an hour). Finally, the third one is related to the ^{214}Pb and ^{214}Bi decay chain that decreases quickly. It is well described by Bateman's equation. It is expected that the impact of the model will be very important on the estimation of their activities. Monte-Carlo simulations of gamma-ray spectra are then obtained by drawing Poisson realizations.

4.2. Comparisons between the different models

In this section, we aim at evaluating the impact of the temporal models on the estimation of the activities. Figure 3 shows the estimated activities in Bq for each time segment and each model, which allows drawing the following conclusions:

- The model "without time" (b in Figure 3) provides accurate activity estimations for the long-lived radionuclides within the last 3 intervals, where the short-lived radionuclides have vanished. In contrast, it is not able to correctly retrieve the activities of the short-lived radionuclides after the third or fourth intervals, when their activities have very low levels. It is important to point out that the estimated activities may vary significantly in time, since no information about the time dependencies of the activities is used in the unmixing procedure. For example, the activity ^{214}Bi (light green in Figure 3) is estimated correctly in the first 6 or 7 intervals but is completely wrong in the last ones since the radionuclide have almost completely disintegrated.

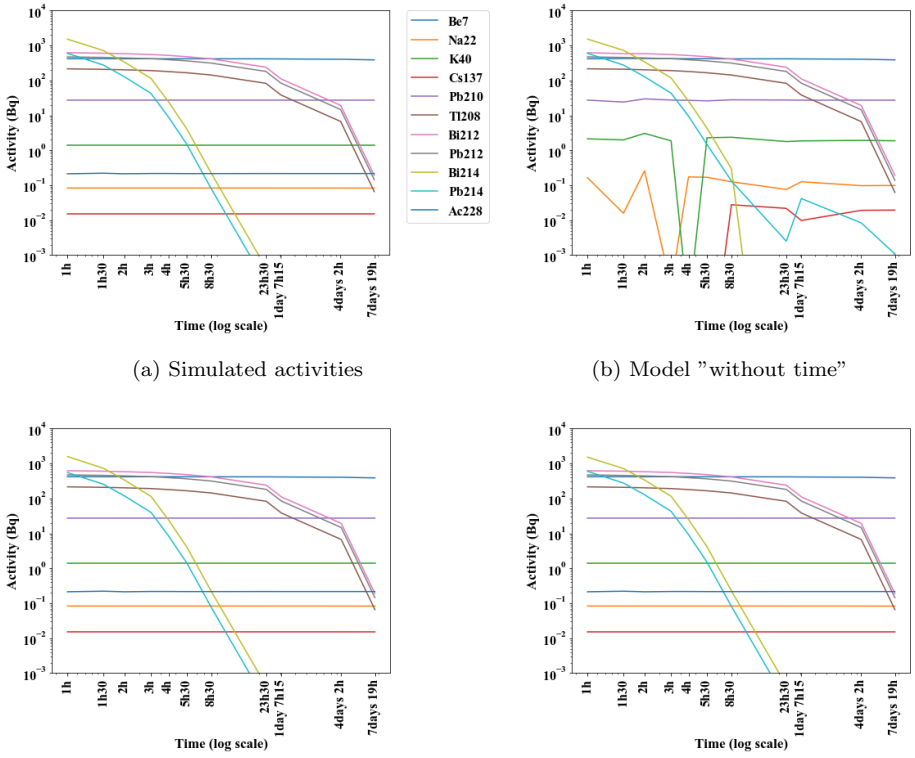

(a) Simulated activities

(b) Model "without time"

(c) Model "Equilibrium hypothesis"

(d) "Bateman" model

Figure 3: Simulated and estimated number of counts per second for the different models and time intervals.

- The two models "Equilibrium hypothesis" and "Bateman", which for time dependencies (c and d in figure 3), yield similar unmixing results. Both give activities' estimates which are close to the ground truth activities.

In order to precisely assess the differences between the unmixing algorithms based on the two temporal models, we propose evaluating experimentally the estimator bias and variance of each method. For that purpose, we applied the unmixing algorithms to 1000 Monte-Carlo simulations of the same mixture.

Figure 4 shows the distribution of the estimated activities for all the 1000 Monte-Carlo simulations, for both Model "Equilibrium hypothesis" (in blue) and "Bateman" model (in orange). These distributions are displayed for 4

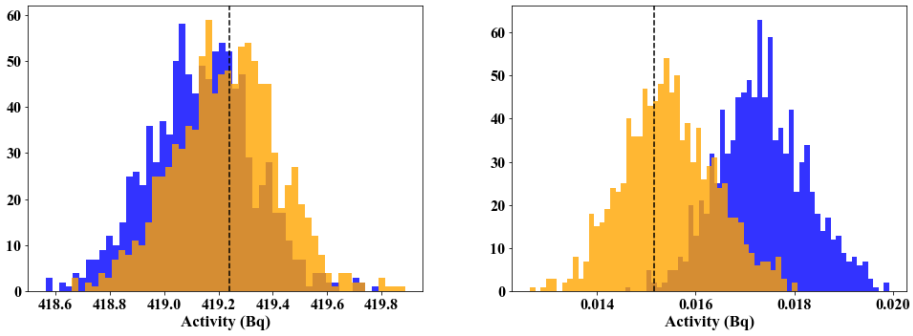

(a) ^{7}Be (b) ^{137}Cs

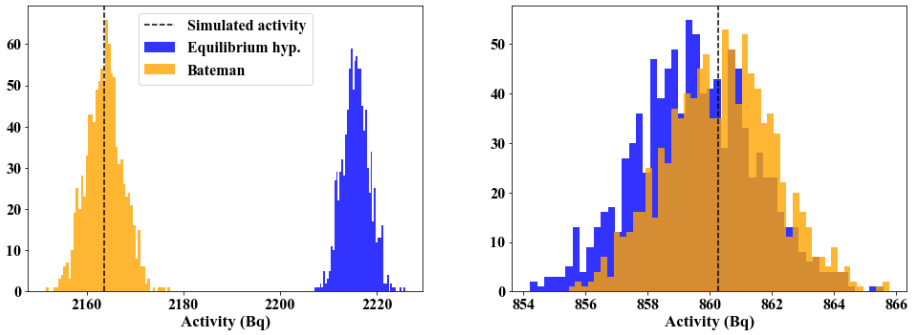

(c) ^{214}Bi (d) ^{214}Pb

Figure 4: Estimated activities by both Model "Equilibrium hypothesis" and "Bateman" for different radionuclides. These graphs are obtained after 10^3 Monte-Carlo simulation.

different radionuclides. For short-lived radionuclides (c and d in figure 4), Model "Equilibrium hypothesis" yields a clear bias, while "Bateman" model provides an unbiased solution. This is especially true for ^{214}Bi. This discrepancy is clearly related to the ability of the "Bateman" model to take into account the correlation in time of the activities of these two radionuclides, which are not in secular equilibrium. More interestingly, for long-lived radionuclides, such as ^{7}Be and ^{137}Cs (a and b in figure 4), the "Bateman" model provides numerically unbiased solutions while Model "Equilibrium hypothesis" yields a slight but statistically significant deviation from the ground truth values. Since these radionuclides have longer half-lives, we would have expected no impact of the

choice of a given time models on the estimated activities. This reveals that i) both models "Equilibrium hypothesis" and "Bateman" use information in all time segments to estimate the activities, and ii) correctly modelling the activity in time of short-lived radionuclides also impacts the activity estimation for radionuclides with longer lives iii) we note that the estimation is not biased if the correct model is taken.

4.3. The role played by temporal information

In this section, we focus on the role played by the temporal information and its impact on activity estimation. For that purpose, we specifically emphasize on the "Bateman" model, which provides a precise description of the time dependencies of the radionuclides' activities. In the following experiment, we propose evaluating the precision of the estimated activities when an increasing number of time intervals are used in the unmixing process. To do so, we start by using only the first interval (i.e. which is similar to take the Model "without time" only for this single interval), then the first two segments, up to all the 11 available time segments. This procedure is also meaningful in the context of crisis, as it allows evaluating how well the radionuclides' activities can be estimated from few and early measurements.

The results are obtained from 1000 Monte-Carlo simulation.

Figure 5 shows the estimated activities of the four radionuclides ^{7}Be (a), ^{137}Cs (b), ^{214}Bi (c) and ^{214}Pb (d). It is interesting to notice that the evolution of the estimated activity of the radionuclides is quite different depending on whether it is a short or long-lived radionuclide.

In case of short-lived radionuclides, such as ^{214}Bi and ^{214}Pb, the relevant information for spectral unmixing is mainly contained in the very first intervals. It entails that the estimated activities of ^{214}Bi and the ^{214}Pb quickly reach a final state. This is also the case for ^{208}Tl, ^{212}Bi and ^{212}Pb, the half lives of which do not exceed 10 hours.

For long-lived radionuclides, the results are slightly different and depends on the activity level. It also depends on how much the presence of short-lived ra-

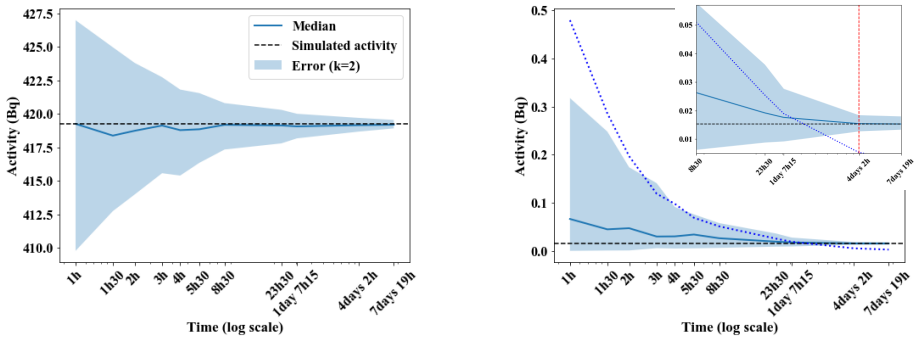

(a) ^{7}Be (b) ^{137}Cs, zoom on the last time segments

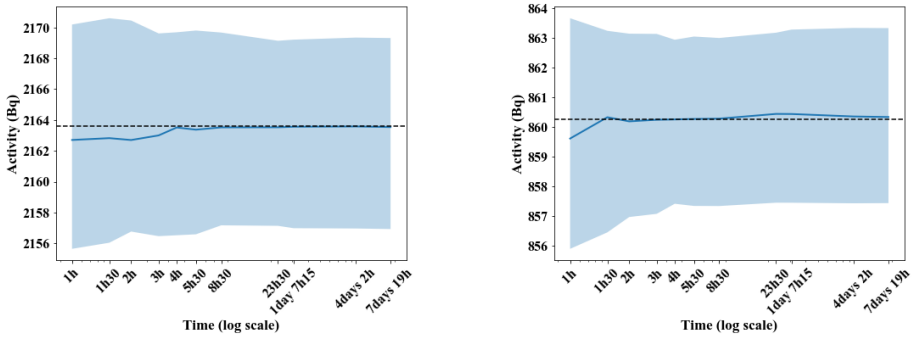

(c) ^{214}Bi (d) ^{214}Pb

Figure 5: Results of the "Bateman" Model on 1000 Monte-Carlo simulations.For ^{137}Cs the decision threshold is presented in dotted blue line.

dionuclides impacts the precision of their activity estimation. For instance, ^{7}Be has a rather high activity and seems less impacted by the presence of short-lived radionuclides. Consequently, its activity is very well estimated already from interval 1 only. In this case, the joint analysis of consecutive time intervals mainly helps improving the uncertainty of the estimation: it naturally decreases as the number of time segments used for the estimation increases.

The case of ^{137}Cs is different since its level is lower (*i.e.* 3 orders of magnitude below the level of ^{7}Be), which makes its activity estimation more sensitive to the presence of short-lived radionuclides. As a consequence, its activity estimation is significantly biased when few time intervals are used. The use of an increasing

number of time intervals helps enhancing both the precision of the estimation and its uncertainty. The estimation of ^{137}Cs is below the decision threshold while the activity of the short-lived radionuclides are predominant but become significant at $t = 1$ day 7h15. It is a significant improvement with respect to previous work Xu et al. (2020), where detection can be claimed at $t = 4$ days 2h as depicted in red on the zoomed plot of figure 5.

In the cases of ^{7}Be and ^{137}Cs, it is important to note that the error decreases with the number of intervals used. Indeed, for these long-lived radionuclides the longer the time segment is and the later it begins, the easier it is to determine their activities. As a result, the statistical error shown in figure 5 decreases for ^{7}Be and ^{137}Cs. On the other hand, the error for short-lived radionuclide like ^{214}Pb and ^{214}Bi is stable from the first segments to the last ones, as their contribution disappears from the spectra after 8 hours of measurement.

5. Application to experimental aerosol measurements

In this section, we analyse a real aerosol sample measurement. This sample is composed of the exact same 11 time intervals we described in table 1 and illustrated in Fig. 1. To that purpose, we apply the proposed unmixing algorithm with the "Bateman" model, being the most realistic when out-of-equilibrium decay series are likely to be present. The experimental protocol is exactly the same as the one used in the simulations. The instrumentation and the radionuclides' signatures are also the same as in the simulations, as described in Appendix A. The background used in the analysis has been measured with the same detector a few weeks after the measurement of the sample, which is the standard laboratory routine.

5.1. Multi-temporal spectral unmixing of an aerosol measurement

In this section, the analysis we performed is exactly the same as in the simulations. Consequently, Figure 6 depicts the evolution of the estimated activities across the different time intervals for ^{7}Be, ^{137}Cs, ^{214}Bi and ^{214}Pb. In this figure,

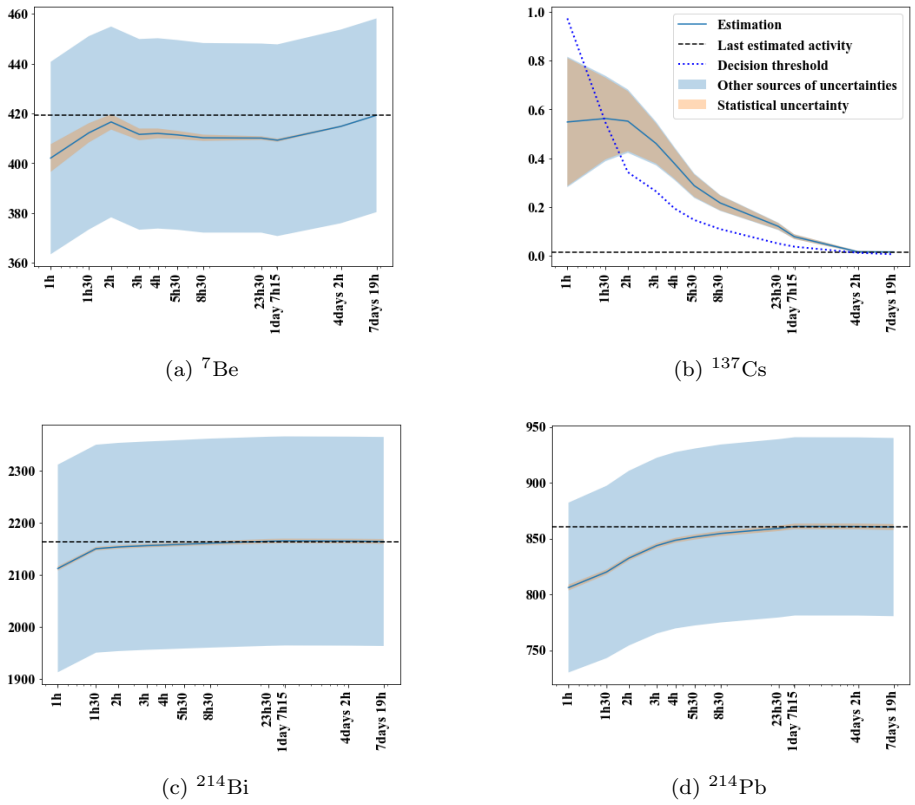

(a) ^{7}Be (b) ^{137}Cs

(c) ^{214}Bi (d) ^{214}Pb

Figure 6: The evolution of the estimation of 4 radionuclides' activity. For ^{137}Cs, the decision threshold is indicated in dotted blue line.

the orange shaded area stands for the statistical error, which originates from the Poisson statistics of the measurements (every errors and uncertainties are taken at 2σ). It is similar to the uncertainty featured in 5. In the previous section (4) this error was computed thanks to Monte-Carlo simulations, this cannot be done on real measurements as the true value of the activities are unknown. The computation of the statistical variability of the estimator is done following the work Xu et al. (2022a), which resorts to the inverse of the Fisher's information matrix of the estimator. If we focus on the estimation of ^{7}Be and ^{137}Cs, the statistical errors for simulations and the real data are similar ($\pm$10Bq for ^{7}Be and $\pm$0.1Bq for ^{137}Cs in the first segment and decreasing as more times seg-

ments are added to the estimation) in both figures. For ^{214}Pb and ^{214}Bi the statistical error small and stable from the first time segment to the last as the activity of these short-lived radionuclides is estimated in the first segments and not affected by the last (the activity of ^{214}Bi, for example, is divided by 512 after only 3 hours of measurement as its half life is 20 minutes). In conclusion we can state that the statistical uncertainties behave similar to the ones measured in the simulations.

Following Xu et al. (2022b), the other sources of uncertainty come from the slight variation of the geometry of the sample, its placement on the endcap of the detector, the calibration of the detector. It is represented by the blue shaded area.

A first observation is that the estimated activities, in all time intervals, are compatible with the last estimate within the total uncertainty budget. However, the case of ^{137}Cs is more peculiar as the estimated activity is about 0.6mBq in the first time intervals, which is about 6 times higher than in the simulations. Furthermore, in these time intervals the estimated activities are not compatible with the final estimate, and also way beyond the detection threshold. This suggests that the estimated activity for ^{137}Cs is significantly biased, at least for the first day of measurements.

As this phenomenon is not observed in the simulations, it is very likely that this originates from a deviation between the observed data and the model that describes these data. This points to the accuracy of the simulated spectral signatures $\mathbf{\Phi}$ and the background; both may deviate from the actual spectral signatures and background. Indeed, in contrast to the other radionuclides displayed in Figure 6, ^{137}Cs has a low level, and is likely to be me more impacted by variabilities of the spectral signatures and the background signature.

5.2. Investigating the impact of the background level

In this section, we propose a simple experiment to highlight the impact of the background level on the estimated activities. For that purpose, rather than

fixing the level of the background, it is estimated during the unmixing process. The background is then described, as any radionuclide, with a spectral signature that is added to the library of spectral signatures. A temporal signature is considered, based on the durations of the time intervals. The "Bateman" model now reads as:

$$\forall s = 1, \cdots, S; c = 1, \cdots, c; \quad x_{sc} = \sum_{n+1} a_n \psi_{sn} \phi_{nc} + \phi_{^{214}Bi,c} \psi_s^{(B)} a_{^{214}Pb} \quad (26)$$

Where ϕ_{n+1} is the normalized background spectrum (*i.e.* corresponding to a 1 second measurement), $\psi_{s,n+1}$ is equal to the duration of the s-th time interval and a_{n+1} is the level of the background. This model is called "Free-background". In the unmixing process, the update rules are similar to the ones detailed in Section 3.

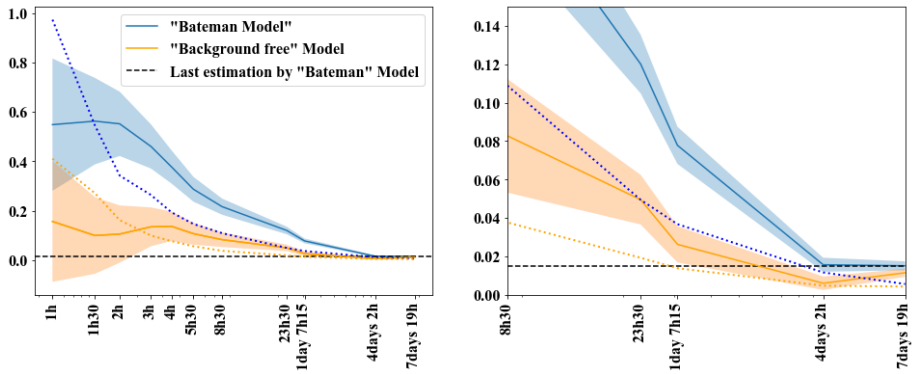

(a) ^{137}Cs (b) Zoom on the last segments

Figure 7: The results for ^{137}Cs with the background treated as a signature (and zoom on the last 4 time segments). The error and decision threshold are depicted in light colour and dotted line, respectively. The black dashed line is the last estimation by the "Bateman" model.

Figure 7 shows the evolution in time of the estimated ^{137}Cs activity for both the standard "Bateman" model and the "Free-background", where the background is estimated. This experiment shows that bias observed in the first time intervals is significantly reduced. The estimated activities during the three first

hours of measurements are now consistent (with respect to the uncertainties) with the final estimated activity. While being reduced, the discrepancy between the final estimate and the ones between 3 hours and 1 day becomes prominent as the statistical uncertainty decreases with time.

The estimated activity of the background is largely superior to 1 on the first 4 segments (estimated to 30 on the 1st-segment-only estimation and decreasing towards 1 between the 1st and the 8th segment).

This first highlights that letting free the background allows capturing some deviation between the data and the original, that could either come from some mis-modelling of the background or the radionuclides'spectral signatures. A simple correction based on the background level is not enough, which suggests that the shape of the spectral signatures should be estimated during the unmixing process.

6. Conclusion

In this article we introduced the full spectrum analysis on multiple spectra which allows accounting for the temporal information of the activity decay in time within the unmixing procedure. For that purpose, we introduce models which are composed of a spectral dictionary and a temporal dictionary. The former contains information about the detectors' response in energy with respect to each radionuclide. The latter is composed of the time decay of each of the radionuclide in the time intervals of the measurements. Two distinct models have been considered: the first one assumes that all the radionuclides are in equilibrium, while the second one allows taking care of parent/daughter dependencies as described by Bateman's equation. We further extended the multiplicative update algorithm to minimise the likelihood of the activities under non-negativity constraints. The proposed algorithms and models have been evaluated and validated on simulations of aerosol samples. These results show that such a method should theoretically yield earlier results for the detection of ^{137}Cs, about one day and a half after sampling, while previous methods re-

quired about four days Xu et al. (2020). The proposed methods have been applied to real measurements of multi-temporal aerosol samples. Though these experiments show the applicability of multi-temporal unmixing for fast activity estimation, the detection and quantification of low-level radionuclides requires understanding the role played by the uncertainty with respect to the background and the radionuclides' spectral signatures. Future investigations will focus on modelling and correcting for these systematics.

Appendix A. Description of the experimental data

In the following, real aerosol filters are sampled in the environment with high volume air samplers, and measured with a High Purity Germanium (HPGe) detector. The experimental set-up consists of a gamma-ray spectrometer with a BEGe 5030 (Broad Energy Germanium, MIRION-Canberra) detector (crystal dimensions: $\emptyset = 80$mm, $h = 30$mm) and a DSA-1000 (MIRION-Canberra) multi-channel analyzer based upon digital signal processing using 16384 channels for energies ranging from 20 keV to 1700 keV. The system has a relative efficiency of 61% and a resolution of 0.54 keV, 1.2 keV and 1.7 keV at 46 keV, 622 keV and 1460 keV, respectively. The detector is surrounded by a 5cm thick lead shield, and equipped by an anti-cosmic set-up consisting in 5 scintillating plastic plates (5 cm thick). Furthermore, the whole system is installed in a shallow shielded room made of 10 cm lead bricks and internally lined by 5 mm oxygen-free copper, in the second basement of the laboratory, under 3 m borated concrete slab. Finally, the inner measurement chamber is flushed by the gaseous nitrogen escaping from the liquid nitrogen dewar to reduce and stabilize the radon induced background. The sampled aerosol filters are pressed into pellets packaged in 10 mL cylindrical counting geometries (dimensions: $\emptyset = 52$mm, $h = 4.7$mm) and measured directly on the detector endcap.

The modeling process of the measurement configuration (detector/counting geometry) as well as the simulations performed to obtain the spectral signatures

used by the spectra unmixing algorithms have been thoroughly described in Xu et al. (2022b). The background spectrum used in the unmixing is considered as constant and perfectly known, and has been experimentally obtained by a background measurement for 560 000 s.

.

References

André, R., Bobin, C., Bobin, J., Xu, J., de Vismes Ott, A., 2020. Metrological approach of gamma-emitting radionuclides identification at low statistics: application of sparse spectral unmixing to scintillation detectors. Metrologia URL: http://iopscience.iop.org/article/10.1088/1681-7575/abcc06.

Bateman, H., 1910. Solution of a system of differential equations occurring in the theory of radio-active transformations. Proc. Cambridge Philos. Soc 15, 423–427.

Chambolle, A., Pock, T., 2011. A first-order primal-dual algorithm for convex problems with applications to imaging. Journal of Mathematical Imaging and Vision 40, 120–145. doi:10.1007/s10851-010-0251-1.

Gilmore, G., 2001. Practical Gamma-ray Spectrometry. Second ed., Wiley-Blackwell.

Hendriks, P., Limburg, J., de Meijer, R., 2001. Full-spectrum analysis of natural γ-ray spectra. Journal of Environmental Radioactivity 53, 365–380. doi:10.1016/S0265-931X(00)00142-9.

Kirkpatrick, J.M., Young, B.M., 2009. Poisson statistical methods for the analysis of low-count gamma spectra. IEEE Transactions on Nuclear Science 56, 1278–1282. doi:10.1109/TNS.2009.2020516.

Knoll, G.F., 2010. Radiation Detection and Measurement. 4th ed., John Wiley & Sons.

Lee, D.D., Seung, H.S., 1999. Learning the parts of objects by nonnegative matrix factorization. Nature 401, 788–791.

Mirion-Canberra, 2016. Genie 2000. URL: https://www.mirion.com/products/genie-2000-gamma-analysis-software.

Sepulcre, Y., Trigano, T., Ritov, Y., 2013. Sparse regression algorithm for activity estimation in γ spectrometry. IEEE Transactions on Signal Processing 61, 4347–4359. doi:10.1109/TSP.2013.2264811.

Sharma, S., Bellinger, C., Japkowicz, N., Berg, R., Ungar, K., 2012. Anomaly detection in gamma ray spectra: A machine learning perspective. doi:10.1109/CISDA.2012.6291535.

de Vismes Ott, A., Gurriaran, R., Cagnat, X., Masson, O., 2013. Fission product activity ratios measured at trace level over france during the fukushima accident. Journal of Environmental Radioactivity 125, 6–16. doi:10.1016/j.jenvrad.2013.02.014.

Xu, J., Bobin, J., de Vismes Ott, A., Bobin, C., 2020. Sparse spectral unmixing for activity estimation in γ-ray spectrometry applied to environmental measurements. Applied Radiation and Isotopes 156, 108903.

Xu, J., Bobin, J., de Vismes Ott, A., Bobin, C., Malfrait, P., 2022a. Analysis of gamma-ray spectra with spectral unmixing, part 1: Determination of the characteristic limits (decision threshold and statistical uncertainty) for measurements of environmental aerosol filters. Applied Radiation and Isotopes 182, 110109.

Xu, J., Bobin, J., de Vismes Ott, A., Bobin, C., Malfrait, P., 2022b. Analysis of gamma-ray spectra with spectral unmixing, part 2: Recalibration for the quantitative analysis of hpge measurements. Applied Radiation and Isotopes 182, 110082.

Yoshida, E., Shizuma, K., Endo, S., Oka, T., 2002. Application of neural networks for the analysis of gamma-ray spectra measured with a ge spectrom-

eter. Nuclear Instruments and Methods in Physics Research Section A Accelerators Spectrometers Detectors and Associated Equipment 484, 557–563. doi:10.1016/S0168-9002(01)01962-3.